Induced Circular Dichroism of Benzo[*a*]pyrene-7,8-dihydrodiol 9,10-Epoxide Stereoisomers Covalently Bound to Deoxyribooligonucleotides Used To Probe Equilibrium Distribution between Groove Binding and Intercalative Adduct Conformations†

Padmanava Pradhan,‡,§ Bengt Jernström,⊥ Albrecht Seidel,|| Bengt Nordén,¶ and Astrid Gräslund*,‡

Department of Biophysics, Arrhenius Laboratories, Stockholm University, S-106 91 Stockholm, Sweden, Institute of Environmental Medicine, Division of Biochemical Toxicology, Karolinska Institute, S-171 77 Stockholm, Sweden, Department of Toxicology, University of Mainz, D-551 31 Mainz, Germany, and Department of Physical Chemistry, Chalmers University of Technology, S-412 96 Göteborg, Sweden

Received November 12, 1997

ABSTRACT: Binding conformations of single *anti*-BPDE-N^2-dG adducts in oligonucleotides of varying base composition have been studied by induced circular dichroism (ICD). The sign of the ICD around 350 nm of single-stranded oligonucleotide adducts and the sign of an exciton type of CD component at 260 nm in both single strand and duplex forms of adducts correlate with the absolute configuration of the cyclohexyl moiety of the adduct. Changes in magnitude and sign of the ICD around 350 nm were observed upon duplex formation. The results show that adducts displaying external (minor groove) binding characteristics are associated with a significant positive ICD. Conversely, adducts displaying intercalation binding characteristics were found to have a positive or negative ICD. The magnitude of the ICD is dependent on the sequence context and the particular adduct isomer studied. Duplexes with (+)-*trans*-*anti*-BPDE-N^2-dG in 5′-d(CCTAT**CGC**TATCC) or 5′-d(CCTAT**AGA**TATCC) exhibit a relatively strong positive ICD. In contrast, the duplexes with (+)-*trans*-*anti*-BPDE-N^2-dG in 5′-d(CCTAT**TGC**TATCC) and 5′-d(CCTAT**TGT**TATCC) display a small positive and negative ICD, respectively, in both cases suggesting conformational heterogeneity. Partially complementary duplexes (dA, dT, or dG) localized opposite the (+)-*trans*-*anti*-BPDE-N^2-dG adduct in 5′-d(CCTAT**CGC**TATCC) or 5′-d(CCTAT**AGA**TATCC) also demonstrated negative ICD. These results together with light absorption characteristics suggest a preferred conformation of intercalation for the mismatched duplexes. Evidence of an equilibrium between the external and intercalative adduct conformation is provided by the results from the temperature dependence of the near-UV absorption and ICD characteristics of (+)-*trans*-*anti*-BPDE-N^2-dG complex in a 5′-d(CCTAT**AGA**TATCC) duplex.

Circular dichroism (CD) spectroscopy can be used to detect interactions of achiral chromophores with chiral moieties. It is well-known that achiral chromophores such as acridine, proflavine, and methylene blue display induced circular dichroism (ICD) upon binding to DNA (*1*−*4*). The ICD induced in the region of the near-UV absorption band of the bound chromophore can provide information about binding geometry and helix conformation (*5*−*8*).

Benzo[*a*]pyrene (BP), a ubiquitous environmental contaminant, is mutagenic and carcinogenic following metabolic activation to diol epoxide intermediates (*anti*- and *syn*-benzo[*a*]pyrenediol epoxide (BPDE) diastereomers and their corresponding enantiomers) and subsequent covalent binding of these electrophiles to DNA (*9*−*12*; see Chart 1). The great difference in biological activity between different BPDE isomers has generated considerable interest in the structural features of their DNA adducts (*13*−*19*). The exocyclic amino groups of the purine bases, viz., the N^2 and N^6 exocyclic amino groups of guanine and adenine, respectively, in native DNA, are the primary targets for adduct formation (*20*). BPDE adduct conformation in well-defined oligonucleotides has been studied by use of (i) optical spectroscopy (*21*−*27*), (ii) high-resolution NMR spectroscopy (*19*), and (iii) computation methods (*28*, *29*). BPDE adduct conformations have traditionally been classified as type I or type II conformations depending on the extent to which the absorption maxima of the duplex in the near-UV region are shifted (*14*, *15*, *22*). Type I conformations with significant pyrene-base stacking interactions display a 5−10-nm shift toward longer wavelength relative to the corresponding BP tetraol and are considered to be of intercalative nature. In type II conformations, the pyrenyl residues are located in

† This work was supported by grants from the Swedish Natural Science Research Council and the Carl Trugger Foundation to A.G., the Swedish Tobacco Company to B.J., and the Deutsche Forschungsgemeinshaft (SFB 302) to A.S.

* Corresponding author: Department of Biophysics, Arrhenius Laboratories, Stockholm University, S-106 91 Stockholm, Sweden.
‡ Stockholm University, Stockholm.
§ Presently on leave from Bio Organic Division, Bhabha Atomic Research Centre, Mumbai, 400 085, India.
⊥ Karolinska Institute, Stockholm, Sweden.
|| University of Mainz, Germany.
¶ Chalmers University of Technology, Göteborg, Sweden.

S0006-2960(97)02783-9 CCC: $15.00
Published on Web 03/13/1998

Chart 1: Structures of the Different Stereoisomers of BPDE-N^2-dG-DNA

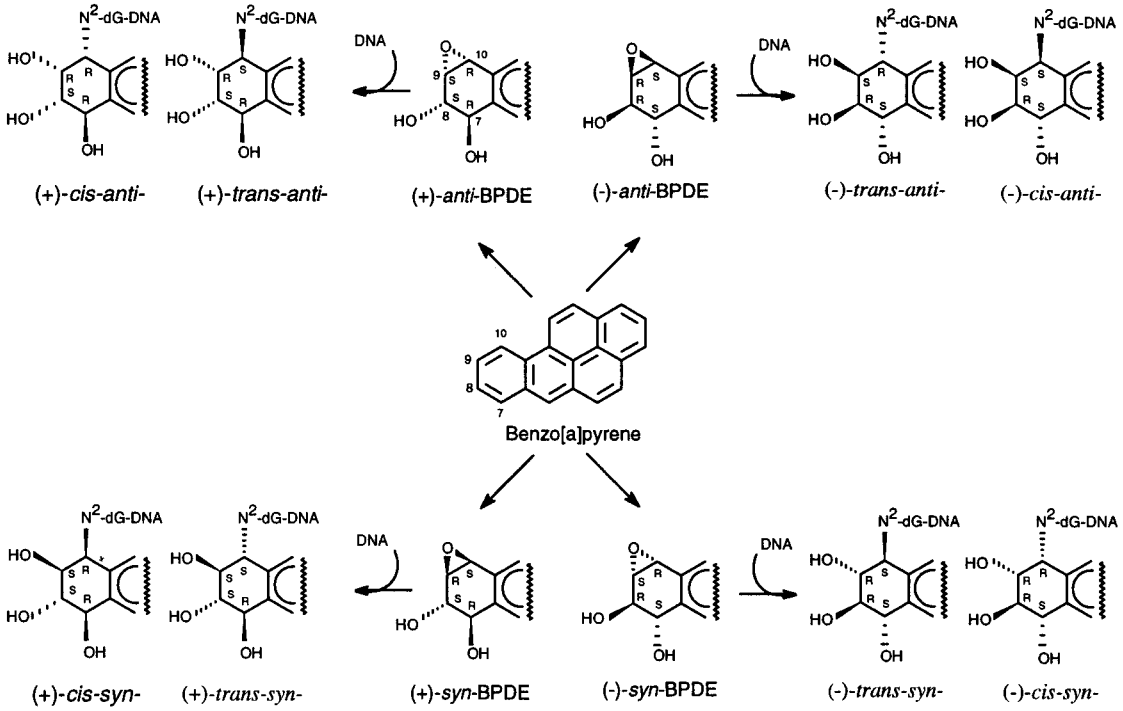

the minor groove (solvent-exposed) and the shift in absorption maxima toward longer wavelength is less pronounced (2−3 nm). In some cases these classifications have been verified by analysis of the solution structures of BPDE adducts using high-resolution NMR (*19*).

The NMR solution structures of the major adducts derived from *anti*-BPDE in the oligonucleotides 5′-d(CCAT**CGC**TACC)/3′-d(GGTAGCGATGG) (*30*) and 5′-d(CCTATG**TGC**AC)/3′-d(GGATACACGTG) (G in bold indicates the adduct site) (*31*) have been determined. In both these structures of the (+)-*trans-anti*-BPDE-N^2-dG adducts and in the structure of the (−)-*trans-anti*-BPDE adduct in 5′-d(CCAT**CGC**TACC)/3′-d(GGTAGCGATGG) (*32*) the majority of the pyrenyl chromophores are localized in the minor groove. In the former case [(+)-*trans-anti*-BPDE, 10*S* absolute configuration] the chromophore is directed toward the 5′-end of the modified strand, whereas in the latter case [(−)-*trans-anti*-BPDE, 10*R* absolute configuration] the chromophore is oriented toward the 3′-end. Depending on the base sequence, viz., in 5′-d(CCTATG**TGC**AC)/3′-d(GGATACACGTG), the (+)-*trans-anti*-BPDE-N^2-dG adduct may also adopt a minor conformation compatible with intercalative binding (*31*).

The solution structures of (+)-*cis-anti*-BPDE (10*R* absolute configuration) and the (−)-*cis-anti*-BPDE adduct (10*S* absolute configuration) in 5′-d(CCAT**CGC**TACC)/3′-d(GGTGCGATGG) have also been determined (*33*, *34*). The predominant conformations of the (+)-*cis*- and (−)-*cis-anti*-BPDE-N^2-dG adducts are characterized by intercalative binding associated with base displacement and are thus different from the major stereoisomeric *trans* adducts.

Situations where a single oligonucleotide adduct may exist in an equilibrium between different conformational states are notoriously difficult to study by NMR and analysis by light absorption spectroscopy only may be ambiguous. In these cases circular dichroism (CD), in particular induced circular dichroism (ICD), may provide further information on adduct conformation and possible heterogeneity.

In the present study a number of oligonucleotides have been specifically modified with the (+)- or (−)-*anti*-BPDE and the *cis*- and *trans*-BPDE-N^2-dG adducts have been analyzed by light absorption spectroscopy and CD. We have focused on adducts in a sequence context previously studied with high-resolution NMR in order to see if the specific structural features of a particular adduct are reflected in the ICD spectrum. To probe the usefulness of ICD in predicting heterogeneity in adduct distribution the technique has also been employed on a few selected adducts with unknown structures. The results show that in the clear-cut cases and even in a case where NMR data have suggested the presence of a minor conformation (*35*), ICD and light absorption indeed reflect the NMR determined adduct structures. These results also indicate that in cases where structural heterogeneity might preclude detailed NMR studies, UV results alone may be ambiguous, but ICD is able to resolve the heterogeneity and suggest the nature of the conformational equilibrium.

MATERIALS AND METHODS

Caution. Benzo[*a*]pyrenediol epoxides are carcinogenic and mutagenic agents and should be handled with care, as outlined in National Cancer Institute Guidelines.

Chemicals. The BPDE diastereomers and their enantiomers were synthesized as described previously (*27*). Oligonucleotides (13-mers) were obtained from Kebo, Stockholm, Sweden. Prior to use their purity was checked by HPLC (see below).

Synthesis and Isolation of BPDE-Modified Oligonucleotides. Single-stranded oligonucleotides [5′-d(CCTAT**XGY**TATCC), where X or Y can be dA, dC, or dT] (100−200 μM) dissolved in 50 mM Tris-HCl, 5 mM EDTA, pH 7.5, were reacted with a 5-fold excess of the (+)- or (−)-

enantiomer of *anti*-BPDE (dissolved in DMSO, final concentration 8.5%). The reaction was allowed to proceed overnight on ice. The reaction mixture was extracted with ethyl acetate to remove the tetraols, the hydrolysis products of BPDE. The remaining organic solvent was removed by a gentle stream of N_2 bubbling through the sample. The extent of overall modification was calculated from the maximal absorbance of the BPDE chromophore at 346−354 nm using $\epsilon = 28.5\ mM^{-1}\ cm^{-1}$. The BPDE-modified oligonucleotides were isolated by semipreparative HPLC as described (*24*, *27*). Acetonitrile was removed from the isolated fractions under a stream of N_2 gas. Subsequently the samples were passed through Sep-Pak C_{18} cartridges (Water associates, Milford, MA) previously washed with methanol (7 mL) and equilibrated with distilled water (2.5 mL). Following application of the samples, 3 × 1 mL of water was allowed to pass the cartridge followed by 3 × 1 mL of methanol to elute the BPDE-modified oligonucleotide.

In the following only the three central bases of the modified oligonucleotides will be referred to, since the flanking bases on either side of the adduct site were not varied.

Preparation of the Tetraols of BPDE. The pure (+)- and (−)-enantiomers of *anti*-BPDE were hydrolyzed to tetraols in dilute HCl. The *cis* and the *trans* isomers formed were separated by HPLC using a reversed phase column (Dynamax 5μ C_{18}, 300-Å pore size, 2.5 × 250 mm i.d., Rainin Instrument Co., Woburn, MA) at 37 °C and a solvent system composed of a linear gradient of 15−50% acetonitrile in ammonium acetate buffer, pH 4.9. After removal of the acetonitrile the fractions containing the tetraols were extracted with ethyl acetate, dried under N_2, and dissolved in 50 mM Tris-HCl buffer, pH 7.5, containing 100 mM NaCl and 5 mM EDTA.

Circular Dichroism. CD spectra of the BPDE-modified oligonucleotides in single-stranded form (dissolved in 50 mM Tris-HCl buffer, pH 7.5, containing 100 mM NaCl and 5 mM EDTA) were recorded on a JASCO spectropolarimeter at 5 °C. The corresponding spectra of the duplexes were measured after addition of the complementary strand followed by at least 1-h storage. The concentrations of the modified oligonucleotides were in the order of 2.5−7 μM in the case of the *trans*-N^2-dG adducts and 1−5 μM in the case of the *cis*-N^2-dG adducts. The concentrations of the tetraols used for CD measurements were in the order of 5−11 μM.

The various contributions to the CD spectrum expected for BPDE-modified oligonucleotides can be summarized as follows: (*1*) intrinsic CD of BPDE due to asymmetric perturbation of the pyrenyl chromophore by the chirally substituted cyclohexyl ring, giving rise to asymmetric static and dynamic contributions of CD to the pyrenyl chromophore, (*2*) intrinsic CD of DNA due to excitonic interactions between stacked nucleotide bases and, to a lesser extent, coupling with far UV transitions of the deoxyribose moieties, (*3*) an exciton type of contribution due to interaction between the transition moments of DNA (260 nm) and the near-degenerated B_b transition moment of the BPDE chromophore, and (*4*) induced CD (ICD) of BPDE adducts due to the coupling between the transitions of the pyrenyl residue and the transitions of the chirally arranged adjacent nucleotide bases.

Table 1: UV (300−400 nm) Absorption Maxima of BPDE-N^2-dG Modified Oligonucleotide in Single-Stranded and Duplex Forms Dissolved in 50 mM Tris-HCl Buffer, pH 7.5, 5 mM EDTA and 100 mM NaCl

adduct	modified sequence[a]	complement	λ_{max} single strand	λ_{max} duplex
(+)-*trans-anti*	CGC	GCG	350, 334, 321	346, 330, 316
		GAG		355, 338
		GTG		354, 339
(+)-*trans-anti*	TGC	GCA	352, 336, 321	346, 330, 315
(+)-*trans-anti*	AGA	TCT	352, 336, 322	346, 330, 316
		TAT		350, 334, 320
		TTT		352, 336, 321
		TGT		352, 335, 321
(+)-*trans-anti*	TGT	ACA	350, 333, 319	347, 331, 317
(−)-*trans-anti*	CGC	GCG	351, 335	347, 330, 316
(+)-*cis-anti*	CGC	GCG	354, 337	355, 340
(−)-*cis-anti*	CGC	GCG	351, 336	355, 338

[a] The three nucleotides at the center of the sequence 5′-d(CCTAT-XXXTATCC) or at its complementary strand.

For B-form DNA, ligand or adduct ICD can be divided into two classes: (a) groove-localized chromophores show strong positive ICD from transition moments oriented along the groove; (b) intercalated chromophores may show weaker positive or negative ICD (*5*, *7*).

For example, for a BPDE adduct localized in the minor groove with the pyrenyl L_a transition moment (∼312, 330, and 350 nm) oriented parallel to the groove, the L_a bands are predicted to exhibit positive ICD and a spectral feature similar to the L_a band (*7*). For the perpendicularly oriented transition moment B_b (∼267 and 277 nm), which is then radially oriented relative to the helix axis and parallel to the planes of the nucleotide bases, only a weak ICD is expected. For intercalated chromophores, in the idealized case when an adduct is positioned near the center of DNA, ICD is negative for the transition moments parallel to the longest dimension of the base-pair intercalation pocket and positive for the orientations parallel to the pseudo-dyad axis (the short axis of the intercalation pocket). In this case, the magnitude of ICD and in some cases also the sign depend not only on the location but also on the orientation of the adduct in the intercalation pocket. If one of the transition moments of the intercalator is oriented with a nonzero angle relative to the longest dimension of the base pair, the magnitude of the ICD can be large.

RESULTS

To probe the usefulness of the ICD method, we have mainly focused our studies on adducts in such sequences where solution structures by NMR have been determined (Tables 1 and 2).

Absorption Spectra of BPDE-Modified Oligonucleotides. The UV absorption spectrum in the 300−400-nm region of BPDE-modified oligonucleotides in single- or double-stranded form was registered (Table 1). The light absorption spectrum of (+)-*trans-anti*-BPDE-N^2-dG adduct in 5′-d(**CGC**) is shown in Figure 1a as an example. The

Table 2: ICD of BPDE-N^2-dG ($\Delta\epsilon$ in M^{-1} cm^{-1}) Modified Oligonucleotide at 5 °C in Single-Stranded and Duplex Forms Dissolved in 50 mM Tris-HCl Buffer, pH 7.5, 5 mM EDTA, and 100 mM NaCl

adduct	absolute configuration	modified sequence	tetraol stereoisomer		adduct				duplex contribution[a]	NMR structure
					single strand		duplex			
			$\lvert\lambda_{max}\rvert$	ICD, M^{-1}	$\lvert\lambda_{max}\rvert$	ICD, M^{-1}	$\lvert\lambda_{max}\rvert$	ICD, M^{-1}	ICD, M^{-1}	
(+)-*trans-anti*	7*R*,8*S*,9*R*,10*S*	CGC	343	−3.1	350	−10.4	347	+5.4	+8.5	minor groove, 5′-orientation[e]
		CGC[b]					354	−17.1	−14.0	
		CGC[c]					352	−31.8	−28.7	
(+)-*trans-anti*		TGC	343	−3.1	350	−4.9	353	−1.9	+1.2	minor groove, 5′-orientation[f]
(+)-*trans-anti*		AGA	343	−3.1	350	−15.8	345	+7.6	+10.7	minor groove, 5′-orientation[g]
		AGA[b]					351	−9.5	−6.4	
		AGA[c]					352	−9.4	−6.3	
		AGA[d]					352	−16.5	−13.4	
(+)-*trans-anti*		TGT	343	−3.1	350	−11.8	355	−10.8	−7.8	
(−)-*trans-anti*	7*S*,8*R*,9*S*,10*R*	CGC	343	+3.8	349	+8.3	345	+9.9	+6.1	minor groove, 3′-orientation[h]
(+)-*cis-anti*	7*R*,8*S*,9*R*,10*R*	CGC	342	+4.1	355	+0.7	354	+22.2	+18.1	base-displaced intercalation[i]
(−)-*cis-anti*	7*S*,8*R*,9*S* ,10*S*	CGC	343	−6.7	353	−1.3	355	+1.1	+7.8	base-displaced intercalation[j]

[a] Obtained by subtracting the ICD of the corresponding tetraol at ∼343 nm from the observed ICD of the modified duplex. [b,c,d] Mismatched duplexes with either dA, dT, or dG, respectively, opposite the modified dG. [e] See reference *30*. [f] With additional minor intercalated conformer (*31*). [g] Minor conformation observed (*35*). [h] See reference *32*. [i] Modified with additional minor conformer of groove binding characteristics (*33*). [j] With additional minor conformer of groove binding characteristics (*34*).

measurements were generally carried out at 15 °C, which is well below the melting temperature (T_m > 35 °C) of the modified duplexes. It can be concluded from Table 1 that all the *anti*-BPDE-N^2-dG oligonucleotide adducts studied exhibit near-UV absorption maxima in single-stranded (ss) form ranging from 350 to 354 nm. Upon addition of the complementary strands to *trans-anti*-BPDE-N^2-dG modified sequences, a substantial shift (3−6 nm) of the maxima toward shorter wavelengths was observed. In contrast, duplex formation of oligonucleotides with *cis-anti*-BPDE-N^2-dG adducts resulted in a shift (1−4 nm) of the maxima toward longer wavelength. Upon addition of partially complementary strands in which the complementary dC opposite the (+)-*trans-anti*-BPDE-N^2-dG adduct in 5′-d(**AGA**) or 5′-d(**CGC**) is replaced with dA, dT, or dG, no change or shifts toward longer or shorter wavelength were observed (Table 1).

In previous studies of BPDE-N^2-dG adducts, optical spectroscopic techniques (*14*−*16*) have been employed to distinguish two types of binding sites, one with intercalative characteristics (type I) and one with external binding (type II) characteristics. This classification has recently been confirmed by high-resolution NMR studies on *anti*-BPDE-N^2-dG adducts in 5′-d(**CGC**) and 5′-d(**TGC**) containing oligonucleotide duplexes (*19*). In this context the terms site I type and site II type have been used. Available evidence shows that *cis-anti*-BPDE-N^2-dG adducts belong to the first category (I), whereas the corresponding *trans* adducts belong to the second category (II).

Circular Dichroism Measurements on Adducts with Known Structures. CD measurements were carried out on single- and double-stranded oligonucleotides containing *trans* and *cis* adducts derived from the (+)- and (−)-enantiomers of *anti*-BPDE (Table 2). As an example the CD spectrum of (+)-*trans-anti*-BPDE-N^2-dG in 5′-d(**CGC**) is shown in Figure 1b. The *trans* adduct is known to be homogeneous and localized in the minor groove (*30*). Figure 2 shows the CD spectrum of (+)-*trans-anti*-BPDE-N^2-dG in 5′-d(**TGC**). As suggested by the results of Fountain and Krugh (*31*) the adduct in 5′-d(**TGC**) may adopt different conformations but the major adduct is localized in the minor groove.

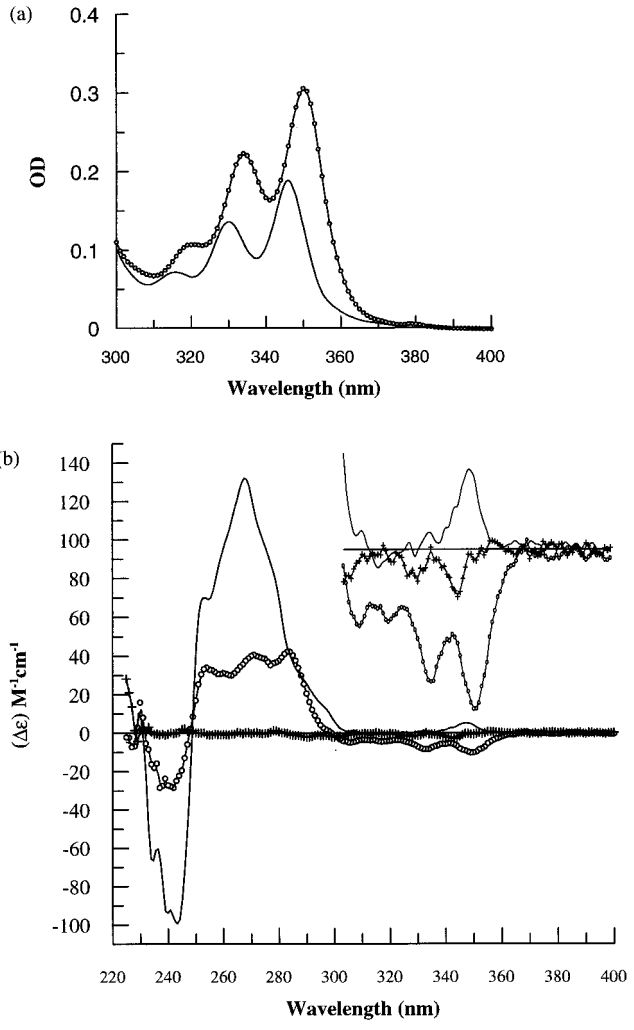

FIGURE 1: (a) UV absorption and (b) CD spectra of (+)-*trans-anti*-BPDE-N^2-dG in 5′-d(**CGC**) in single-stranded (○) and duplex (—) forms at 5 °C in 50 mM Tris-HCl buffer, 100 mM NaCl, and 5 mM EDTA, pH 7.5. The CD spectrum of the corresponding tetraol isomer is also included (+). Concentration of adduct and corresponding tetraol isomer, 6.7 and 6.8 μM, respectively, 10× higher gain.

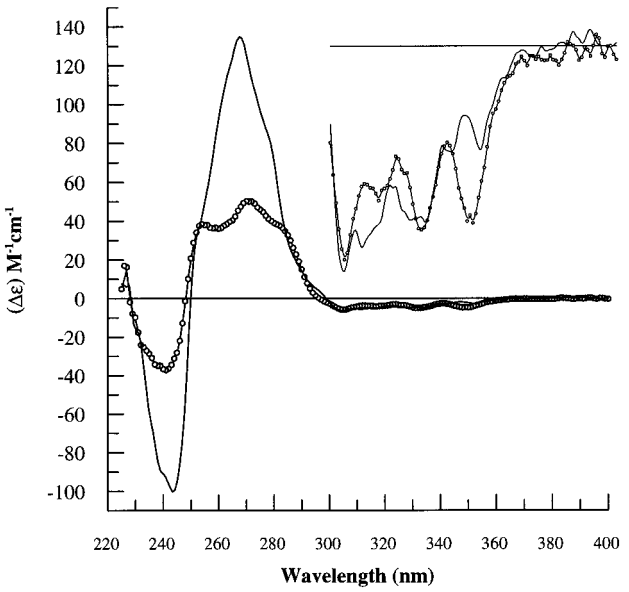

FIGURE 2: CD spectra of (+)-*trans-anti*-BPDE-N^2-dG in 5′-d(**TGC**) in single-stranded (○) and duplex (—) forms. Adduct concentration, 7.0 μM. Other conditions as in Figure 1.

In the exciton CD spectra, the modified oligonucleotides have maxima or minima at 252−260 nm, where the oligonucleotides have strong absorption. The sign of the spectrum depends on the absolute configuration at the benzylic C-10 position of the BPDE adduct in both single- and double-stranded oligonucleotides. The adducts with 10*S* absolute configuration at the C-10 position [e.g., (+)-*trans*- and (−)-*cis-anti*-BPDE-N^2-dG] exhibit a positive CD spectrum around 252−260 nm, whereas the adducts with 10*R* absolute configuration [e.g., (−)-*trans*- and (+)-*cis-anti*-BPDE-N^2-dG] exhibit a negative exciton CD spectrum. Similar findings have been obtained with single nucleotide and nucleoside adducts of BPDE as well as with oligonucleotide adducts (*20*, *22*, *27*, *36*).

The data obtained from the ICD measurements at longer wavelengths with the different adducts are compiled in Table 2. The sign of the ICD in the single-stranded form reflects the absolute configuration at the benzylic C-10 position of the BPDE adduct. The adducts with 10*S* absolute configuration at the C-10 position [e.g., (+)-*trans*- and (−)-*cis-anti*-BPDE-N^2-dG] exhibit a negative ICD spectrum at 346−355 nm, whereas the adducts with 10*R* absolute configuration [e.g., (−)-*trans*- and (+)-*cis-anti*-BPDE-N^2-dG] exhibit a positive ICD spectrum.

The ICD in the region of 300−360 nm should originate from the interaction of the pyrenyl chromophore with the chirally stacked DNA bases and the chiral cyclohexyl moiety of the adduct. To assess the ICD originating from the oligonucleotide−BPDE adduct interaction, the contribution of the cyclohexyl chirality must therefore first be subtracted. To estimate this contribution, ICD spectra were recorded for the (+)-*trans*- and the (+)-*cis-anti*-BPDE-N^2-dG adduct in single-stranded 5′-d(**AGA**) at temperatures ranging from 5 to 75 °C. As shown in parts a and b of Figure 3, respectively, the spectral intensities diminished gradually toward higher temperatures, probably due to decreased base−adduct stacking interactions, but no change in sign was observed. The rate of change of ICD in case of the *cis* adduct was found to be lower than for the *trans* adduct, reflecting stronger pyrene-nucleobase stacking. To further reduce stacking interactions, 20% DMSO was added. A small shift to shorter wavelength was observed, but there was no significant change in intensity (Figure 3c). The high-temperature spectra were found to be very similar to those of the corresponding tetraol.

Typical tetraol ICD spectra are shown in Figure 3c,d. The CD data of the tetraol isomers are included in Table 2 and are fully consistent with those of Weems and Yang (*37*). To estimate the contribution of the oligonucleotide duplex to the ICD of the modified sample, the ICD of the longest wavelength spectral extreme point of the corresponding tetraol was subtracted. The subtractions, with results as shown in Table 2, do not take into account the small wavelength shifts of the spectra.

The ICD of the (+)-*trans-anti*-BPDE-N^2-dG adduct in 5′-d(**CGC**) in the single-stranded form was negative (−10.4 M^{-1}) but changed sign upon duplex formation. The duplex contribution to ICD was found to be positive (8.5 M^{-1}). In this adduct the BP ring is positioned in the minor groove and directed toward the 5′-end of the modified strand (*30*). The ICD of the (+)-*trans-anti*-BPDE-N^2-dG adduct in 5′-d(**TGC**) was also negative (−4.9 M^{-1}) in the single-stranded form. Unlike the (+)- and the (−)-*trans-anti*-BPDE-N^2-dG adducts in 5′-d(**CGC**) where ICD maxima were identical to the near-UV absorption (345−347 nm), the ICD minima (353 nm, Figure 2) and the near-UV maxima (346 nm, Table 1) for the adduct in 5′-d(**TGC**) sequence context were different. The duplex contribution to ICD was found to be weak but positive (1.2 M^{-1}). This adduct has been shown to be heterogeneous in its solution structure, with a major conformer located in the minor groove and a minor conformer intercalated (*31*). For the (+)-*trans-anti*-BPDE-N^2-dG adduct in 5′-d(**AGA**) the ICD of the single strand was negative (−15.8 M^{-1}), with a relatively strong positive duplex contribution (10.7 M^{-1}) (Figure 4). Recent preliminary results from NMR measurements have suggested that the adduct is positioned in the minor groove with 5′-orientation (*35*).

The (−)-*trans-anti*-BPDE-N^2-dG adduct in 5′-d(**CGC**) showed a positive ICD in single-stranded form, becoming further positive in duplex form with a duplex contribution to the ICD of 6.1 M^{-1} (Figure 5). This adduct is also known to be localized in the minor groove with a 3′- orientation (*32*).

The CD spectra of the (+)- and (−)-*cis-anti*-BPDE-N^2-dG adducts in 5′-d(**CGC**) are shown in parts a and b of Figure 6, respectively. These adducts have base-displaced intercalative binding sites (*33*, *34*). Both have weak ICD in single-stranded forms probably reflecting structural disorder. The ICD of the (+)-*cis* adduct had a strong positive duplex contribution (18.1 M^{-1}). The (−)-*cis* adduct had a negative ICD in the single-stranded form but changed sign in the duplex form with a positive duplex contribution of 7.8 M^{-1}.

It can be concluded from Table 2 that both the minor groove localized (+)- and (−)-*trans-anti*-BPDE-N^2-dG adducts in 5′-d(**CGC**) and the (+)-*trans-anti*-BPDE-N^2-dG adduct in 5′-d(**TGC**) exhibit a positive duplex contribution to ICD. It should be noted that the heterogeneous conformations observed by NMR for (+)-*trans-anti*-BPDE-N^2-dG adducts in 5′-d(**TGC**) is reflected in a numerically very small duplex contribution to the ICD. Positive ICD contribution

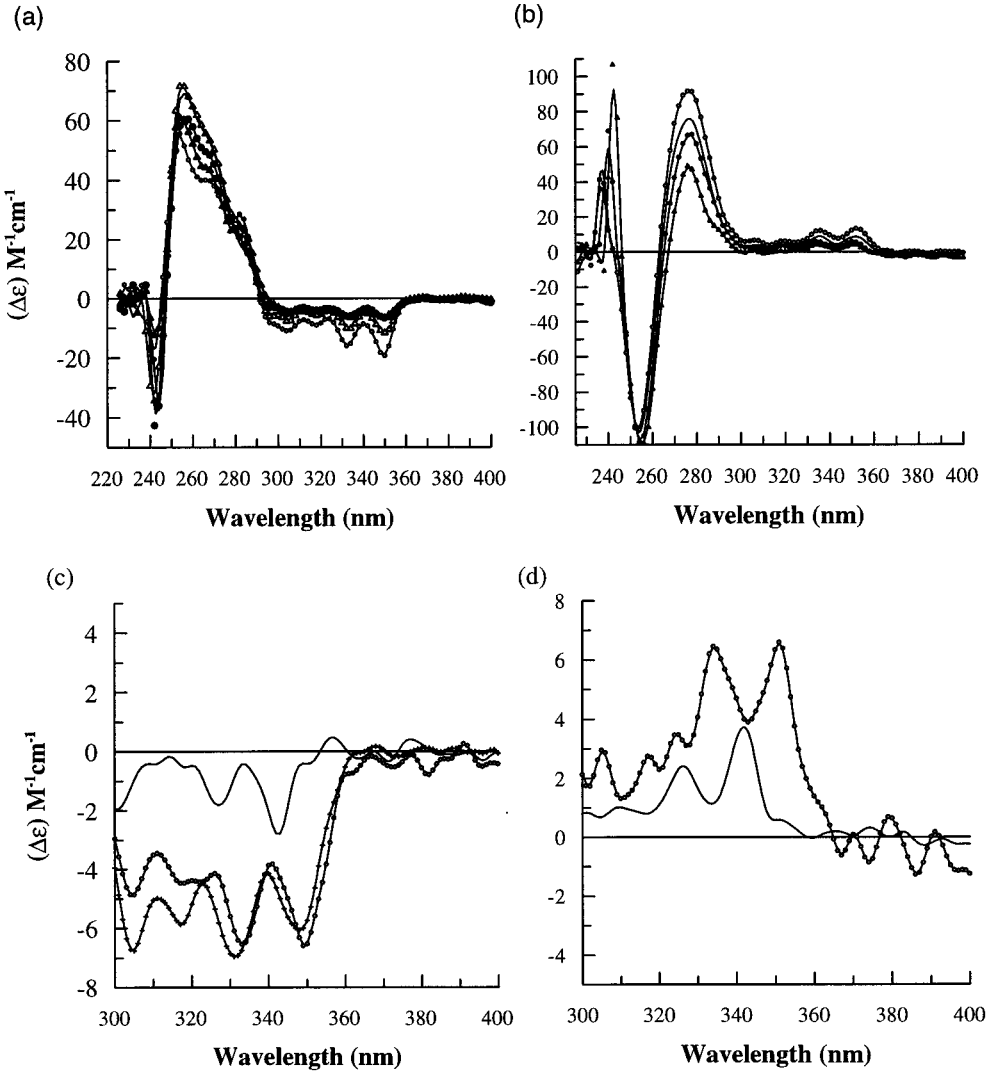

FIGURE 3: ICD of (a) (+)-*trans*- and (b) (+)-*cis*-*anti*-BPDE-N^2-dG in 5′-d(**AGA**) in single-stranded forms at 5 (○), 15 (△), 25 (−), 45 (●), and 75 °C (▲). In (c) and (d), ICD spectra of (+)-*trans*- and (+)-*cis*-*anti*-BPDE-N^2-dG in 5′-d(**AGA**) in single-stranded form (○) at 75 °C are compared with that of the corresponding tetraols (−). The ICD spectrum of the (+)-*trans* adduct in the presence of 20% DMSO at 75 °C (+) is also included in (c). Concentrations of the adducts, 7.3 and 8.7 μM, and those of the corresponding tetraols, 6.8 and 11.3 μM, respectively. The other conditions as in Figure 1.

from duplex formation were observed for the intercalated (+)- and (−)-*cis*-*anti*-BPDE-N^2-dG adducts in 5′-d(**CGC**).

Induced Circular Dichroism of Adducts with Unknown Structures. Figure 4 shows the ICD spectrum of the (+)-*trans*-*anti*-BPDE-N^2-dG adduct in 5′-d(**AGA**) and with matched and mismatched complementary sequences. As previously described and shown in Table 2, the ICD of the single strand adduct is negative and the duplex contribution is positive in a correct complementary sequence. However, when the (+)-*trans*-*anti*-BPDE-N^2-dG adduct is present in mismatched duplexes, the ICD remained negative in all cases (Figure 4). Similarly, with the (+)-*trans*-*anti*-BPDE-N^2-dG in 5′-d(**CGC**) the positive ICD observed with the fully complementary duplex became strongly negative in mismatched duplexes (Figure 1b and Table 2).

Figure 7 shows the CD spectrum of (+)-*trans*-*anti*-BPDE-N^2-dG in 5′-d(**TGT**). Optical spectroscopy studies on the adduct structure characterized this as a site II adduct in 5′-d(CACA**TGT**ACAC) (*22*), but no NMR structure is available. The ICD of this adduct in the present sequence is negative in both single- and double-stranded form. It should also be noted that upon duplex formation the minima of the ICD are shifted to longer wavelengths at 355 nm (cf. Table 2). The UV absorption maximum of the duplex, on the other hand, appeared at 347 nm as expected for minor groove localization of the BPDE-chromophore (Table 1).

UV Absorption and CD as a Function of Temperature. Figure 8a shows the effect of temperature on the UV absorption spectrum (300−350 nm) of the (+)-*trans*-*anti*-BPDE-N^2-dG adduct in double-stranded 5′-d(**AGA**). No change in absorption maxima was observed at temperatures where the duplex is fairly stable (T_m = 38 °C, 100 mM NaCl, 50 mM Tris-HCl, pH 7.5, and 5 mm EDTA). Beyond 30 °C a shift to longer wavelength was observed mainly due to an increasing extent of single strand formation. Figure 8b shows the corresponding ICD spectra at different temperatures. Increasing the temperature from 5 to 45 °C resulted in a gradual change in the ICD from positive values of high magnitude to highly negative values. At temperatures below 30 °C, there was a net positive contribution to the ICD at 347 nm from the oligonucleotide−adduct interaction but it decreased with increasing temperature. Since the results in

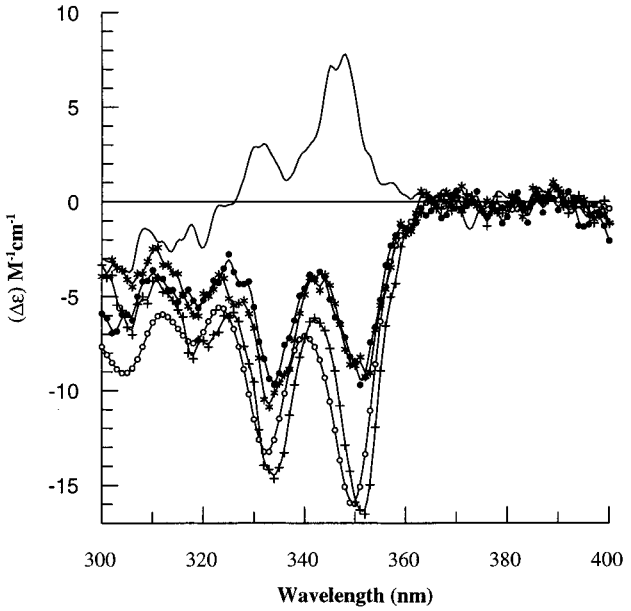

FIGURE 4: Expanded (300−400 nm) ICD spectra of (+)-*trans-anti*-BPDE-N^2-dG in 5′-d(**AGA**) in single-stranded form (○) and with the fully complementary strand (−) or with dA (●), dT (*) and dG (+) opposite the adduct. Adduct concentrations, 2.7 μM in all cases. Other conditions as in Figure 1.

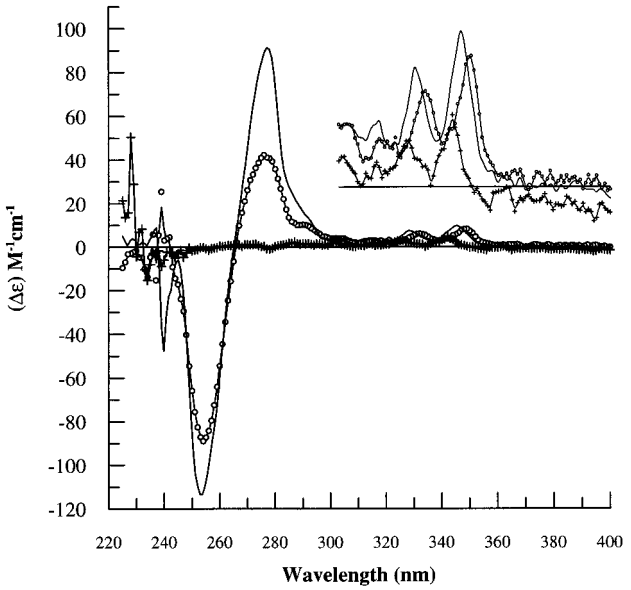

FIGURE 5: CD spectra of (−)-*trans-anti*-BPDE-N^2-dG in 5′-d(**CGC**) in single-stranded (○) and duplex (−) forms. Adduct concentration, 5.1 μM. The CD spectrum of the corresponding tetraol isomer (6.0 μM) is also shown (+). Other conditions as in Figure 1.

Figure 8a clearly indicate that the duplex conformation of the adducted oligonucleotide is intact at least up to 28 °C, the change in ICD should reflect a change in adduct conformation. It is interesting to note that the ICD profile at 30 °C is similar to those for the (+)-*trans-anti*-BPDE-N^2-dG with 5′-d(**TGC**) and 5′-d(**TGT**) sequence contexts at 5 °C (Figures 2 and 7). In each case, there is a negative minimum at a wavelength around 353−356 nm (typical for a type I site) and a negative crest at 346 nm.

DISCUSSION

CD and Absolute Adduct Configuration. For the series of BPDE-N^2-dG adducts studied (Table 2) a definite correlation is noted between the sign of the exciton CD band at 250−260 nm and the absolute configuration of these adducts in both single- and double-stranded oligonucleotides (*20*, *22*, *27*, *38*). Similarly, the sign of the ICD of a particular adduct in a single-stranded oligonucleotide at 350 nm follows the same pattern as the intrinsic CD of the corresponding BPDE tetraol isomer. Irrespective of base sequence context, the (+)-*trans*- and (−)-*cis-anti*-BPDE-N^2-dG adducts with a 10*S* absolute configuration exhibit negative ICD at 346−353 nm in single-stranded forms. In contrast, adducts with 10*R* absolute configuration exhibit positive ICD in this region. Hence, the signs of both CD and ICD can be guidelines in identifying the absolute configurations of BPDE-N^2-dG adducts in oligonucleotides. In a recent study, the ICD of *anti*-BPDE-N^6-dA adducts in the human N-*ras* proto-oncogene was used to assign the absolute configuration of

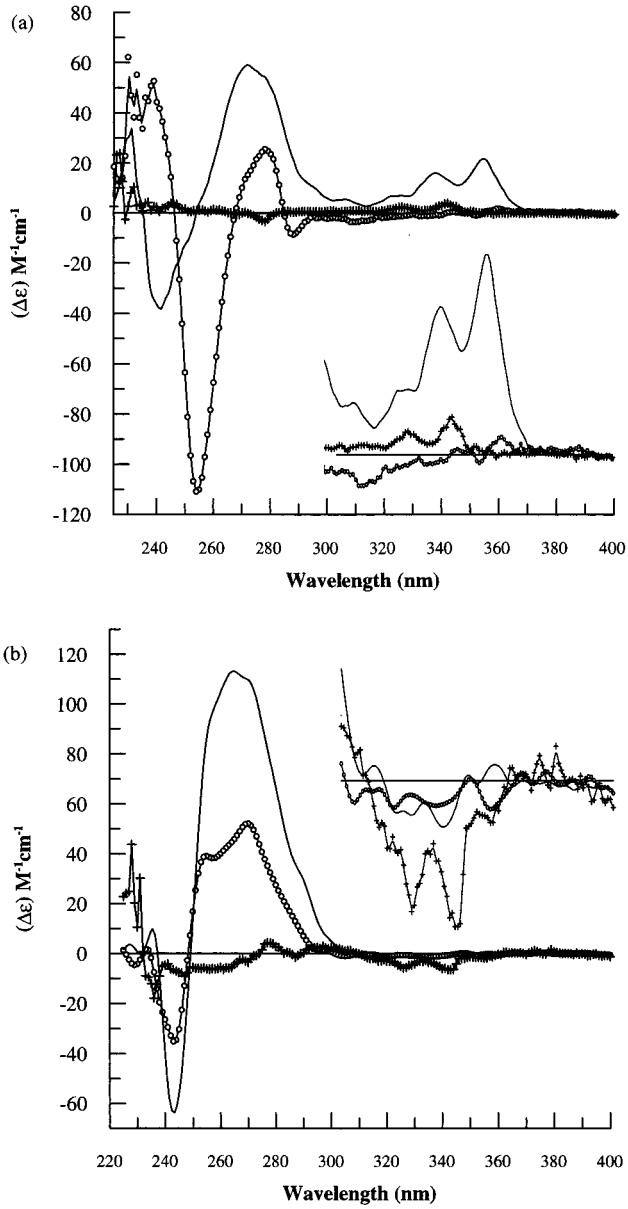

FIGURE 6: CD spectra of (a) (+)-*cis-anti*-BPDE-N^2-dG and (b) (−)-*cis-anti*-BPDE-N^2-dG in 5′-d(**CGC**) in single-stranded (○) and duplex forms (−). The CD spectra of the corresponding tetraol isomers are also included (+). The concentrations of the adducts, 5.6 and 5.2 μM, and of the tetraol isomers, 11.3 and 5.0 μM, respectively. Other conditions as in Figure 1.

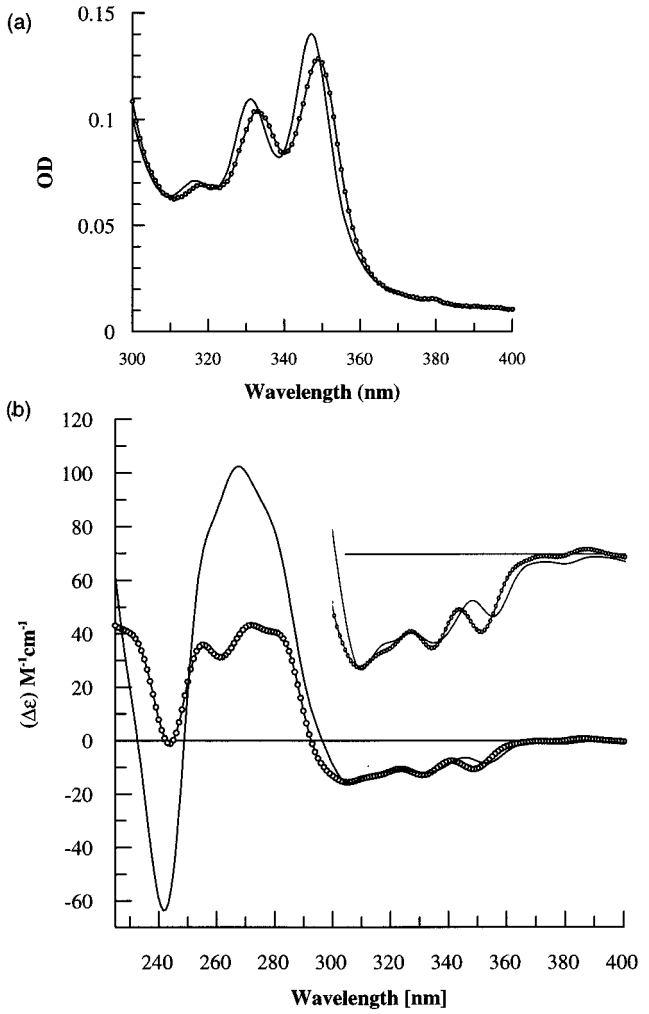

FIGURE 7: (a) UV absorption and (b) CD spectra of (+)-*trans-anti*-BPDE-N^2-dG in 5′-d(**TGT**) in single-stranded (○) and duplex (—) forms. Adduct concentration, 4.2 μM. Other conditions as in Figure 1.

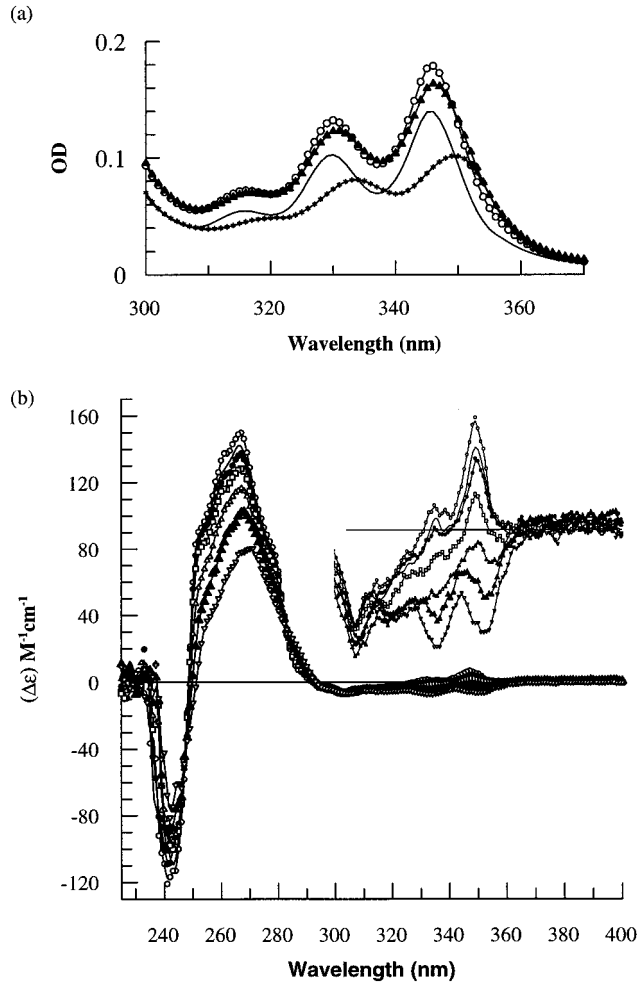

FIGURE 8: (a) Near-UV (300−400 nm) absorption spectra of (+)-*trans-anti*-BPDE-N^2-dG in 5′-d(**AGA**) duplex, T_m = 38, at 4 (—), 20 (○), 28 (▲), and 35 °C (*). (b) CD spectrum of (+)-*trans-anti*-BPDE-N^2-dG in 5′-d(**AGA**) containing oligonucleotide duplex at 5 (○), 15 (—), 20 (●) 25 (□), 30 (△), 35 (▲) and 45 °C (▽). Concentration and other conditions as in Figure 1.

the pyrenyl chromophore (*39*). As is evident from the present study, both the sign of the ICD and its magnitude are highly influenced by the type of adopted adduct conformations and their relative distribution.

ICD of Externally Localized (Site II) Adducts. For the established externally localized minor groove adducts (site II) studied here a positive duplex contribution to the ICD was observed in all cases (Table 2). The magnitudes of ICD were found to differ and depend on the sequence context. Previous results using UV absorption and fluorescence spectroscopy (*27*) as well as preliminary NMR results (*35*) have suggested that the (+)-*trans-anti*-BPDE-N^2-dG adduct in double-stranded 5′-d(**AGA**) has an external localization. The positive ICD of the adduct observed here substantiates this suggestion. A positive ICD was also predicted for groove binders based on complete calculations by the "matrix method" of Schellman and Tinoco *(6, 8)* and an idealized coupled-oscillator model (*5, 7*) for achiral chromophores externally bound to a chiral macromolecule.

The (+)-*trans-anti*-BPDE-N^2-dG adduct in 5′-d(**TGT**) has not previously been well characterized. The UV absorption maximum at 347 nm for the duplex is indicative of a type II conformation (Table 1) (*22*), but the observed ICD with a minimum at 355 nm and with a strong negative duplex contribution (Table 2) is not consistent with this interpretation. A similar discrepancy between UV and ICD spectral extreme points was observed for the (+)-*trans-anti*-BPDE-N^2-dG adduct in 5′-d(**TGC**) (Tables 1 and 2). The latter adduct has been shown to have a conformational distribution, with a dominant minor groove conformer and smaller intercalated one (*31*). We conclude that a similar situation occurs in the 5′-d(**TGT**) conformer, possibly with a larger intercalative fraction reflected in its strong negative duplex ICD (Table 2).

Negative duplex ICD was also observed in mismatched duplexes containing 5′-d(**AGA**) or 5′-d(**CGC**) adducts (Table 3). Although the wavelength shift associated with duplex formation varies, the sign and magnitude of the ICD in single- and double-stranded oligonucleotides are similar in each case. The solution conformations of the adducts in mismatched duplexes may resemble the ones present in duplexes in which deletions opposite the adduct site have been introduced. These duplexes lack proper Watson−Crick base pairing at the adduct site. An NMR solution structure of the (+)-*trans-anti*-BPDE-N^2-dG adduct in 5′-d(CCAT**CGC**-TACC) having a complement lacking the dC opposite to the adduct suggests that the pyrenyl chromophore is intercalated and the modified dG displaced into the major groove (*40*).

A similar study on the (+)-*cis-anti*-BPDE-N^2-dG adduct also suggests intercalative binding and a displacement of the modified dG, but in this case into the minor groove (*41*). Hence, the present results indicate that the pyrenyl chromophore of (+)-*trans-anti*-BPDE-N^2-dG adduct in mismatched duplexes forms base-displaced intercalating complexes as the major conformational state. This result is also in agreement with the long-wavelength UV absorption above 350 nm (Table 1).

ICD of Intercalated (Site I) Adducts. In general, intercalation is the major conformation of site I adducts. In an idealized case where the intercalator is near the center of DNA, the ICD is negative for transition moments parallel to the longest dimension of the base-pair intercalation pocket and positive for orientations parallel to the pseudo-dyad axis (the short axis of the intercalation pocket) (*4*, *5*, *7*). The magnitude, and in some cases also the sign, depends not only on the orientation but also on the location of the chromophore in the intercalation pocket. In many site I adducts the modified dG is displaced from the center of the helix toward the major or the minor groove and hence may have a stronger contribution to the magnitude of the ICD (*8*). The *cis* adducts of (+)- or (−)-*anti*-BPDE in 5′-d(**CGC**) with known base displaced intercalated structures and positive duplex ICD are examples of this category (Table 2). For these adducts we observe similar shifts to longer wavelengths in the UV absorption and ICD spectra.

External−Internal Adduct Conformer Interchange. Previous studies have provided evidence that a single BPDE adduct in oligonucleotide duplexes can adopt different conformations and that their relative conformer distribution is dependent on the base sequence (*25*, *31*, *26*, *19*). Such a heterogeneous conformer distribution was earlier predicted on the basis of results from linear dichroism and fluorescence spectroscopy experiments on BPDE-modified polydeoxyribonucleotides (*15*, *25*). A decrease of the linear dichroism amplitude of DNA itself has been ascribed to a decreased persistence length of the double helix, owing either to increased flexibility ("flexible joints") or to permanent kinks at the points of BPDE modification (*42*). The linear dichroism of BPDE could be fitted to a bimodal conformational distribution having the long axis of the pyrenyl residue at a small angle (minor groove orientation) or a large angle (intercalation). Theoretical considerations as well as experimental results show that the N^2-dG adducts derived from several BPDE enantiomers can be rearranged from minor groove localization (*19*) to a base-displaced intercalation site.

Effect of Temperature on Conformer Distribution. The ICD of (+)-*trans-anti*-BPDE-N^2-dG in 5′-d(**AGA**) varies markedly with temperature from positive to negative values with increasing temperature (Figure 8). At temperatures well below T_m (38 °C), the decrease in ICD is probably due to a shift in the conformational equilibrium. NMR studies on (+)-*trans-anti*-BPDE-N^2-dG in 5′-d(**AGA**) displayed similar results (*35*). The NMR spectrum displayed two imino resonances for the modified dG whose relative intensities varied with change in temperature, thus reflecting two conformations in slow exchange. It should be noted that the ICD at 30 °C is similar to those of the (+)-*trans-anti*-BPDE-N^2-dG adducts in 5′-d(**TGC**) and 5′-d(**TGT**) sequence contexts at 5 °C. As the (+)-*trans-anti*-BPDE-N^2-dG adduct in 5′-d(**TGC**) is known to have an additional minority conformation (*31*), the same can be predicted for the (+)-*trans-anti*-BPDE-N^2-dG adduct in 5′-d(**TGT**) and that in 5′-d(**AGA**) sequence at higher temperature. With increasing temperature the contribution to ICD of adducts in single-stranded form will become more pronounced and hide the effects of a conformer rearrangement.

Effect of Flanking Bases on Adduct Conformational Distribution. When a (+)-*trans-anti*-BPDE-N^2-dG adduct is present in 5′-d(**CGC**) or 5′-d(**AGA**) the magnitude of the duplex ICD is strongly positive. However, the duplex contribution to ICD of the (+)-*trans-anti*-BPDE-N^2-dG oligonucleotides is found to be small and postive, e.g., 5′-d(**TGC**), or negative, e.g., 5′d(**TGT**), whenever the 5′-flanking base adjacent to the adduct is dT. The smaller magnitude of the ICD in the above cases indicates an increase in heterogeneity of adduct conformations, possibly due to the weaker Watson−Crick pairing for TA pairs than for the other base pairs on the 5′- flank of the lesion site. Results from NMR spectroscopy (*31*) also show that the presence of a 5′-dT adjacent to the adduct site increases the heterogeneity of adduct conformations. Experimental results using alternating and nonalternating polynucleotides have shown that the distribution of external and intercalative adduct localization is strongly dependent on sequence context. For instance, in 5′-d(**GGG**) and 5′-d(**CGC**) external localization greatly dominates, whereas in 5′-d(**AGA**) and 5′-d(**TGT**) the contribution of intercalative binding becomes increasingly more important (*43*).

CONCLUSION

As demonstrated in this study, ICD provides a valuable tool to study the conformational distribution of PAH−DNA adducts and appears to provide additional structural information to that obtained by other optical spectroscopic methods (*14*, *15*, *19*, *25*). BPDE-N^2-dG adducts in oligonucleotide duplexes with UV $\lambda_{max} < 350$ nm that exhibit a significant duplex-induced positive ICD in the near-UV absorption region of the pyrenyl moieties have a minor groove location (site II) as the predominant conformation. The net duplex contribution to the ICD is dependent on the sequence context of the oligonucletides. BPDE-modified duplexes of this type, generally with a dT flanking the adduct, which exhibit a small positive or negative contribution to ICD have adduct heterogeneity. The heterogeneity is manifested in noncoinciding extreme points of the long-wavelength UV and ICD spectra. BPDE-N^2-dG adducts in oligonucleotide duplexes with UV $\lambda_{max} > 350$ nm that exhibit either positive or negative contributions to the ICD have intercalated binding (site I) as the predominant conformation. Mismatched duplexes with the (+)-*trans-anti*-BPDE-N^2-dG adduct show a negative ICD, consistent with a predominantly intercalative (site I) conformation. The distribution of adduct conformations has been demonstrated to be temperature dependent, a factor which has already been assumed to partially influence the mutational spectra induced by the (+)-*anti*-BPDE-dG adducts (*44*) and, therefore, to be of great importance for biological systems.

ACKNOWLEDGMENT

We thank Dr. Ingrid Pontén for helpful comments and providing some of the BPDE-modified samples. The excel-

lent technical assistance of Kerstin Ström is also gratefully acknowledged.

REFERENCES

1. Neville, D. M., Jr., and Bradley, D. F. (1961) *Biochim. Biophys. Acta 50*, 497−399.
2. Nordén, B., and Tjerneld, F. (1977) *Chem. Phys. Lett. 50*, 508−512.
3. Fornaseiro, D., and Kuruscev, T. (1981) *J. Phys. Chem. 85*, 613−618.
4. Nordén, B., and Tjerneld, F. (1982) *Biopolymers 21*, 1713−1734.
5. Schipper P. E., Nordén, B., and Tjerneld, F. (1978) *Chem. Phys. Lett. 8*, 1−15.
6. Lyng, R., Härd, T., and Nordén, B. (1987) *Biopolymers 26*, 1327−1345.
7. Kubista, M., Åkerman, B., and Nordén, B. (1988) *J. Phys. Chem. 92*, 2352−2356.
8. Lyng, R., Rodger, A., and Nordén, B. (1991) *Biopolymers 31*, 1709−1720.
9. Gelboin, H. (1980) *Physiol. Rev. 60*, 1107−1166.
10. Conney, A. H. (1982) *Cancer Res. 42*, 4875−4917.
11. Cooper, C. S., Grover, P. L., and Sims, P. (1983) *Prog. Drug Metab. 7*, 295−396.
12. Thakker, D. R., Yagi, H., Levin, W., Wood, A. W., Conney, A. H., and Jerina, D. M. (1985) in *Bioactivation of Foreign Compounds* (Anders, M. W., Ed.) pp 177−242, Academic Press, New York.
13. Jeffrey, A. M. (1985) in *Polycyclic Hydrocarbons and Carcinogenesis* (Harvey, R. G., Ed.) ACS Symposium Series 283, pp 187−208, American Chemical Society, Washington, DC.
14. Geacintov, N. E. (1985) in *Polycyclic Hydrocarbons and Carcinogenesis* (Harvey, R. G., Ed.) ACS Symposium Series 283, pp 107−124, American Chemical Society, Washington, DC.
15. Gräslund, A., and Jernström, B. (1989) *Quart. Rev. Biophys. 22*, 1−37.
16. Geacintov, N. E., Cosman, M., Ibanez, V., Birke, S. S., and Swenberg, C. E. (1990) in *Molecular basis of specificity in nucleic acid-drug interactions* (Pullman, B., and Jortner, J., Eds.) pp 433−449, Kluwer Academic Publishers, Netherlands.
17. Jerina, D. M., Chadha, A., Cheh, A. M., Schurdak, M. E., Wood, A. W., and Sayer, J. M. (1990) in *Biological Reactive Intermediates IV. Molecular and cellular effects and their impact on human health* (Wittmer, C. M., Snyder, R., Jollow, D. J., Klaf, G. F., Kocsis, J. J., and Snipes, I. G., Eds.) pp 533−553, Plenum Press, New York.
18. Jernström, B., and Gräslund, A. (1994) *Biophys. Chem. 49*, 185−199.
19. Geacintov, N. E., Cosman, M., Hingerty, B. E., Amin, S., Broyde, S., and Patel, D. J. (1997) *Chem. Res. Toxicol. 10*, 111−146.
20. Cheng, S. C., Hilton, B. D., Roman, J. M., and Dipple, A. (1989) *Chem. Res. Toxicol. 2*, 334−340.
21. Cosman, M., Ibanez, V., Geacintov, N. E., and Harvey, R. G. (1990) *Carcinogenesis 11*, 1667−1672.
22. Geacintov, N. E., Cosman, M., Mao, B., Alfano, A., Ibanez, V., and Harvey, R. G. (1991) *Carcinogenesis 12*, 2099−2108.
23. Mao, B., Xu, J., Li, B., Margulis, L. A., Smirnov, S., Ya, N.-Q., Courtney S. H., and Geacintov, N. E. (1995) *Carcinogenesis 16*, 357−365.
24. Pontén, I., Kim, S. K., Gräslund, A., Nordén, B., and Jernström, B. (1994) *Carcinogenesis 15*, 2007−2213.
25. LeBreton, P. R., Huang, C.-R., Fernando, H., Zajc, B., Lakshman, M. K., Sayer, J. M., and Jerina, D. M. (1995) *Chem. Res. Toxicol. 8*, 338−348.
26. Suh, M., Ariese, F., Small, G. J., Jankowiak, R., Liu, T.-M., and Geacintov, N. E. (1995) *Biophys. Chem. 56*, 281−296.
27. Pontén, I., Seidel, A., Gräslund, A., Nordén, B., and Jernström, B. (1996) *Chem. Res. Toxicol. 9*, 188−196.
28. Singh S. S., Hingerty, B. E., Singh, U. C., Greenberg, J. P., Geacintov, N. E., and Broyde, S. (1992) *Cancer Res. 51*, 3482−3492.
29. Kozack, R. E., and Loechler, E. L. (1997) *Carcinogenesis 18*, 1585−1593.
30. Cosman, M., de los Santos, C., Fiala, R., Hingerty, B. E., Ibanez, V., Margulis, L. A., Live, D., Geacintov, N. E., Broyde, S., and Patel, D. J. (1992) *Proc. Natl. Acad. Sci. U.S.A. 89*, 1914−1918.
31. Fountain, M. A., and Krugh, T. R. (1995) *Biochemistry 34*, 3152−61.
32. de los Santos, C., Cosman, M., Fiala, R., Hingerty, B. E., Ibanez, V., Margulis, L. A., Geacintov, N. E., Broyde, S., and Patel, D. J. (1992) *Biochemistry 31*, 5245−5252.
33. Cosman, M., de los Santos, C., Fiala, R., Hingerty, B. E., Ibanez, V., Luna, E., Harvey, R. G., Geacintov, N. E., Broyde, S., and Patel, D. J. (1993) *Biochemistry 32*, 4145−4155.
34. Cosman, M., Hingerty, B. E., Luneva, N., Amin, S., Geacintov, N. E., Broyde, S., and Patel, D. J. (1996) *Biochemistry 35*, 9850−9863.
35. Pradhan, P., Jernström, B., and Gräslund, A. (1997) NMR Solution Structure of the (+)-trans-anti-benzo[a]pyrene-7,8-dihydrodiol-9,10-epoxide-deoxyguanosine adduct in a 5′-d(CCTATAGATATCC)/3’-d(GGATATCTATAGG) oligonucleotide duplex, in *Nordic NMR Symposium*, Abstract, p 71, Carlsberg Laboratory, Copenhagen, Denmark.
36. Canella, K. A., Peltonen, K, Yagi, H, Jerina, D. M., and Dipple, A. (1992) *Chem. Res. Toxicol. 5*, 685−690.
37. Weems, H. B., and Yang, S. K. (1989) *Chirality 1*, 276−283.
38. Sayer, J. M., Chadha, A., Agarwal, S. K., Yeh, H. J. C., Yagi, H., and jerina, D. M. (1991) *J. Org. Chem. 56*, 20−29.
39. Chaturvedi, S., and Lakshman M. K. (1996) *Carcinogenesis 17*, 2747−2752.
40. Cosman, M., Fiala, R., Hingerty, B. E., Luneva, N., Amin, S., Geacintov, N. E., Broyde, S., and Patel, D. J. (1994) *Biochemistry 33*, 11507−11517.
41. Cosman, M., Fiala, R., Hingerty, B. E., Luneva, N., Amin, S., Geacintov, N. E., Broyde, S., and Patel, D. J. (1994) *Biochemistry 33*, 11518−11527.
42. Eriksson, M., Nordén, B., Jernström, B., and Gräslund, A. (1988) *Biochemistry 27*, 1213−1221.
43. Roche, C. J., Jeffrey, A. M., Mao, B., Alfano, A., Kim, S. K., Ibanez, V., and Geacintov, N. E. (1991) *Chem. Res. Toxicol. 4*, 311−317.
44. Rodriguez, H., and Loechler, E. L. (1993) *Biochemistry 32*, 1759−1769.

BI972783F